Flatband Potential of F:SnO_2 in a TiO_2 Dye-Sensitized Solar Cell: An Interference Reflection Study

M. Turrión,[†] J. Bisquert,*[,‡] and P. Salvador*[,§]

Instituto de Estructura de la Materia, CSIC, Serrano 113 bis, 28006 Madrid, Spain, Departament de Ciències Experimentals, Universitat Jaume I, 12080 Castelló, Spain, and Instituto de Catálisis y Petroleoquímica, CSIC, Spain

Received: March 27, 2003; In Final Form: May 28, 2003

A model for the analysis of interference reflection data of nanoporous TiO_2 dye-sensitized solar cells (DSSC) is presented. It is shown that the interference reflection technique [Turrión, M.; Macht, B.; Tributsch, H.; Salvador, P. *J. Phys. Chem. B* **2001**, *105*, 9732] allows one to monitor very precisely the evolution of the depletion layer of the fluor-doped SnO_2 (FTO) conducting substrate at the DSSC back contact with the position of the Fermi level. The model shows that this technique features a much larger sensitivity than the capacitance−voltage Mott−Schottky method for determining both the flatband potential (U_0) and the Helmholtz layer capacitance (C_H) at the FTO/electrolyte interface, under working conditions of the DSSC. Under illumination the band-bending in the FTO substrate is controlled by two factors: (a) the position of Fermi level (FTO bulk potential), which is determined by the accumulation of photogenerated electrons in the conduction band of the nanostructured TiO_2 film, and (b) the values of U_0 and C_H, which determine the potential distribution at the FTO/electrolyte interface. It is suggested that both parameters U_0 and C_H determine a constraint on the maximum photovoltage attainable by the DSSC, as the conduction band edge of the FTO at the FTO/TiO_2 interface cannot be higher than that of the TiO_2, otherwise the transfer of dye photoinjected electrons from the TiO_2 to the FTO would be hindered. According to our analysis, it can be concluded that the theoretical maximum photovoltage cannot be higher than 0.8 V, a value never surpassed experimentally with untreated DSSC.

1. Introduction

Fluor-doped SnO_2 (FTO) is a highly doped semiconductor frequently used as a transparent back contact in photovoltaic devices such as TiO_2 dye-sensitized solar cells (DSSC). FTO is generally considered as a degenerate semiconductor (metallic behavior), where the external applied bias drops at the Helmholtz layer. However, this is far from being true, since due to its low dielectric contact ($\epsilon_r = 9$), even when highly doped ($N_d = 10^{21}$ cm^{-3}), FTO has a non-negligible electric field region (depletion layer) at its interface with the electrolyte, which can be modulated under external bias.[1−3]

The external potential applied to a DSSC is placed at the FTO/TiO_2 interface (back contact), generating there an externally modulable electrical potential barrier that is able to hinder the injection in the dark of electrons from the FTO substrate to the TiO_2 and to promote the transfer of photoinjected electrons from the TiO_2 to the FTO.[4,5] The energy structure of this potential barrier is very important in determining the behavior of the DSSC both in the dark and under illumination. Some authors have suggested that the photopotential of a DSSC arises from the compensation under illumination of the FTO/TiO_2 electrical potential barrier existing under equilibrium conditions in the dark, which means that the maximum attainable photopotential should be limited by the height of this barrier.[6] However, this hypothesis seems to contradict certain experimental evidence about the modification of the DSSC photopotential by treatment of the TiO_2 surface.[7] More plausible seems to be the model according to which the photopotential is a consequence of the build-up of photoinjected electrons at the TiO_2 conduction band, which raises the DSSC Fermi level under open circuit conditions.[1,5] In any case, any reliable model for describing the photopotential of a DSSC must take into account the actual structure of the potential barrier at the FTO/TiO_2 back contact. Recent works have emphasized the existence of a reverse barrier for electrons flowing from TiO_2 toward the contact,[8] where recombination increases.[9] We will show that this barrier strongly depends on the built-in potential at the FTO/electrolyte interface, U_0 (a more extended definition of U_0 will be given in section 4).

The flatband potential conventionally obtained from Mott−Schottky plots, when measured with respect to the counter electrode of the DSSC, corresponds to $-U_0$. However, a precise determination of U_0 by these methods is not possible. At potentials more positive than the flatband potential, the FTO/electrolyte interface provides the main contribution to the photoelectrode capacitance.[10] Due to the electrical characteristics of the FTO layer (high N_d and low ϵ_r), the specific capacitance associated with its space charge region, C_b, has the same order of magnitude as the Helmholtz layer capacitance, C_H, and, although the Mott−Schottky (MS) (C^{-2} vs V plot) remains linear[11−15] and its slope does not change, the x-axis intercept is

* Corresponding authors. E-mail: (J.B.) bisquert@uji.es, (P.S.) dmipss9@ps.uib.es.
[†] Instituto de Estructura de la Materia.
[‡] Universitat Jaume I.
[§] Instituto de Catálisis y Petroleoquímica. Present address: Departament de Matemàtiques i Informàtica, UIB, 07071 Palma de Mallorca, Spain.

10.1021/jp034774o CCC: $25.00
Published on Web 07/26/2003

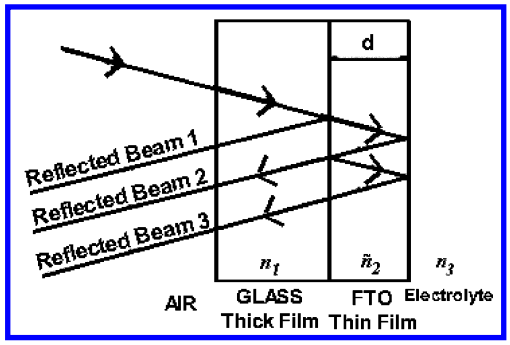

Figure 1. Schematic diagram of the optic path of the light through the system (air/glass/FTO/electrolyte). d is the FTO film thickness.

shifted toward negative potential values with respect to the flatband potential, by an amount[11]

$$U_1 = \frac{N_d e \epsilon_r \epsilon_0}{2C_H^2} \tag{1}$$

in such a way that an apparent flatband $-(U_0 + U_1)$ is obtained. Since U_1 is very sensitive to C_H and the actual value of C_H is not generally known, a large uncertainty results in the determination of the flatband potential from MS analysis.

Another important question is the need for in situ characterization of the flatband potential under DSSC working conditions, with intense illumination in the experimental sandwich configuration. In this respect, previous studies of unsensitized nanostructured TiO_2 (without dye) revealed a major anodic shift of the flatband potential, nearly 0.5 V, under UV illumination. This was interpreted as an effect of band edge movement in the nanostructured material by trapping of minority carriers (holes) in surface states.[16]

Besides electrolyte electrorreflectance, the interference reflection technique is an alternative and powerful experimental method very sensitive to the magnitude of the electric field at the FTO depletion layer.[1] In this paper we develop a new method for an in situ precise estimation of the potential distribution at the FTO/electrolyte interface of the DSSC back contact from experimental interference reflection data, under working conditions of the solar cell. It will be shown that both U_0 and U_1 (and hence C_H) constitute independent parameters that can be determined with a high accuracy. Important implications of the FTO band-edge shift, which takes place during illumination of the DSSC under open circuit conditions, on the theoretically attainable maximum photovoltage will also be analyzed.

2. Interference Reflection Spectra

The interference reflection technique is based on a well-defined modulation reflection spectrum due to a multiple interference process originated at the FTO transparent conducting substrate of the DSSC back contact.[1] The interpretation of the interference reflection spectra in thin oxide films has been corroborated by various authors,[17−19] as a perturbation of the complex optical dielectric constant of the film. In this section we discuss the derivation of theoretical spectra resulting from such perturbation in the FTO thin film.

The interference reflection spectrum of a system built by three phases with different refraction indexes (glass/FTO/electrolyte) depends mainly on the complex refraction index of the thin film of FTO, $\hat{n}_2(\lambda)$; see Figure 1.

The reflectance R is described by taking into account the multiple reflection effect within the FTO film as the product of

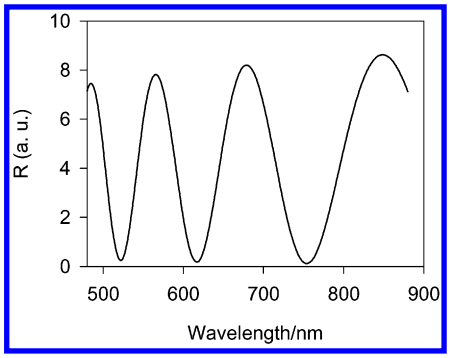

Figure 2. Reflection spectrum given by eq 5. $n_1 = 1.5$, $n_2 = 2.12$, $n_3 = 1.52$, $k_2 = 0.02$, $d = 800$ nm.

the reflection coefficient multiplied by its conjugate complex,[20]

$$R(\hat{n}_2(\lambda)) = \rho\rho^* = \left|\frac{r_1 + r_3\gamma}{1 + r_1 r_3 \gamma}\right|^2 \tag{2}$$

where r_1 and r_3 are the complex reflection coefficients in the interfaces glass/FTO and FTO/electrolyte, respectively, and γ is the complex phase difference. The reflection coefficient of both interfaces can be expressed either as a module and a phase or by means of their respective refraction indexes,

$$r_1 = m e^{i\delta} = \frac{n_1 - \hat{n}_2}{n_1 + \hat{n}_2} \quad r_3 = n e^{i\delta'} = \frac{n_3 - \hat{n}_2}{n_3 + \hat{n}_2} \tag{3}$$

Here, n_1 and n_3 are the refraction indexes of the glass and electrolyte, respectively. The factor γ represents the exponential of the complex difference of phase due to the difference in the optical path of the reflected light in both interfaces,

$$\gamma = \exp\left[\frac{4\pi i}{\lambda}\int_0^d \hat{n}_2 dx\right] = \exp\left[\frac{4\pi i d}{\lambda}(n_2 + ik_2)\right] = \exp[-x' + ix] \tag{4}$$

where d is the film thickness and λ the wavelength of the incident light. Replacing eqs 3 and 4 in 2, we can obtain the reflectance,

$$R = \frac{m^2 e^{x'} + n^2 e^{-x'} + 2mn\cos(\delta' - \delta + x)}{e^{x'} + m^2 n^2 e^{-x'} + 2mn e^{-x'}\cos(\delta' + \delta + x)} \tag{5}$$

Figure 2 represents the interference reflection spectrum given by eq 5.

The absorption coefficient depends quadratically on the local field $E(x)$,[18,19] so that the perturbation of $\hat{n}_2$ may be written as

$$\Delta\hat{n}_2 = i\frac{\lambda}{2\pi}C(\lambda)E\Delta E \tag{6}$$

where $C(\lambda)$ is a coefficient that depends on the shape of the modulated reflection spectrum. The differential reflectance ΔR can be obtained from eq 2 as

$$\Delta R = 2\mathrm{Re}\left[\frac{1 - r_1^2}{1 - r_1 r_3 \gamma^2}\rho(\gamma\Delta r_3 + r_3\Delta\gamma)\right] \tag{7}$$

The change in r_3 is given by

$$\Delta r_3 = \frac{-2n_1}{(n_1 + \hat{n}_2)^2}\Delta\hat{n}_2 \tag{8}$$

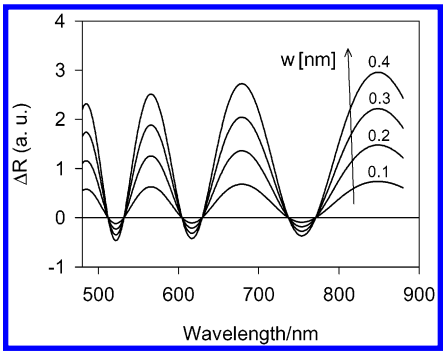

Figure 3. Modulated reflectance spectra calculated from eq 7 for different dc applied bias, inducing the following values of the FTO depletion layer thickness $w = 0.1$, 0.2, 0.3, 0.4 nm. A value of $b = 1$ and an invariant line shape were assumed in eq 9.

Assuming a linear field profile in the FTO film across the space charge region, w (see eq 10 below), it is easily shown with the help of eq 6 that the modulation of r_3 depends only on the modulation amplitude (V_{ac}) and not on the dc bias. So, the effect of the electric field on the difference of optical path of the light can be expressed as

$$\Delta\gamma = \mathrm{i}\frac{4\pi}{\lambda}\gamma\int\Delta\hat{n}_2 dx = C(\lambda)bV_{ac}w \qquad (9)$$

where b is a constant. Similar results have been obtained in ref 18.

The contribution to the modulated reflectance of the term $\Delta\gamma$ depends on both the amplitude of the modulation and with the dc bias. In the present case, like in the results presented by Blackwood and Peter,[19] the potential dependence of $\Delta R/R$ shows that the second contribution is the dominant one.

Figure 3 represents the modulation reflectance spectra under application of different dc potentials, obtained from eq 7, by taking into account eqs 6, 8, and 9.

3. Experimental Section

The results reported here were obtained[1] with a DSSC in the standard sandwich-type configuration in which a dyed nanoporous TiO_2 electrode is facing a Pt counter electrode. The FTO conductive glass substrates (Solems Z. I. Les Glaises) had a thickness of about 3 mm (FTO thickness $\approx 0.8\,\mu$m) and a square resistance of 9 Ω. A thin film of nanostructured TiO_2 was deposited over the substrate and sensitized with a Ru-complexed dye. A platinized F:SnO_2 sheet (3 nm Pt) was used as a counter electrode. The cell was filled with organic electrolyte (acetonitrile, 0.5 M LiI, 50 mM I_2, 0.2 M 4-tertbutylpyridine) and sealed with Surlyn 1702-Dupont. The DSSC was illuminated from the FTO side with a 150 W Xe lamp followed by a monocromator (Oriel Corp.). Interference effects involving multiple reflections in the FTO were observed using the experimental set up previously described.[1]

Figure 4 shows the influence of the dc applied bias on the modulation reflection spectra of the DSSC. According to eq 7 and Figure 3, our model attributes the behavior observed in Figure 4 to the fact that an important part of the dc external bias (V_{dc}) drops at the depletion region of the FTO, modifying its band-bending.[1] Therefore, we will assume in the following that the modulation of the reflectance is dominated by the term associated with the light transmitted through the FTO.

In principle, the interference effects in thin films could be due either to modulation of the optical constants or to field-induced changes in film thickness (electrostriction). The calculation presented by Blackwood and Peter[19] leads us to think that the electrostrictive effect is not responsible for the observed spectra. Blackwood and Peter calculated the electrostriction effect in oxide films on Ti and they observed that the form and the position of the maxima and minima in the spectrum changed with the applied field. Our experimental spectra in Figure 4 do not correspond to this behavior, as we observe that the intensity of the signal changes with the applied field but not its form nor the position of the maxima and minima. In addition, the calculated spectra are inverted with respect to those observed experimentally. Matthews et al.[21] have shown that the film thickness increases in the presence of an electric film, but in the calculation presented in ref 19, it is necessary to assume that the film thickness decreases rather than increases. Therefore, we concluded that as previously shown for oxide films on titanium[19] the electric field modulation of the optical constants produces the interference effects observed in our experiments.

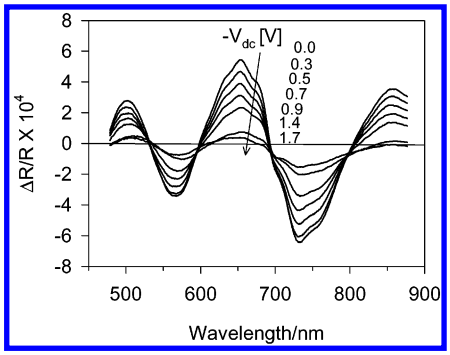

Figure 4. Influence of the dc applied bias V_{dc} (increasing negatively from 0 to −0.3, −0.5, −0.7, −0.9, −1.4, and −1.7 V) on the modulation reflection amplitude, for $V_{ac} = 0.3$ V and a modulation frequency $f = 230$ Hz. $\Delta R/R$ reaches its maximum amplitude for $V_{dc} = 0$ (short circuit conditions), where the band-bending at the FTO conducting substrate is a maximum, and decreases as V_{dc} becomes increasingly negative, i.e., as the Fermi level is pushed upward and the band-bending diminishes.

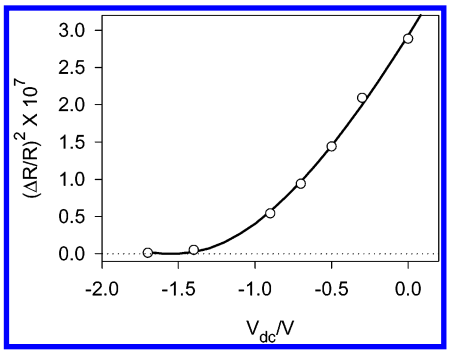

Figure 5. Plot of $(\Delta R/R)^2$ vs V_{dc} for spectra maxima at 1.88 eV of Figure 1. The circles are experimental data and the line the best fit to the model outlined in the text (eq 16).

4. Modulated Reflectivity Dependence on the Applied Potential

Figure 5 shows the experimental dependence of modulated reflection amplitude ΔR on the bias potential from the data of Figure 4. The dependence of $(\Delta R/R)^2$ on V_{dc} in Figure 5 is characterized by an almost linear shape for $V_{dc} > -0.8$ V; for more negative potentials, as the electrode potential approaches the flatband value, the curve bends and tends to flatten.

In this section we show that the behavior indicated in Figure 5 can be explained on the basis of a detailed description of the potential distribution existing at the FTO/electrolyte interface.[2,10]

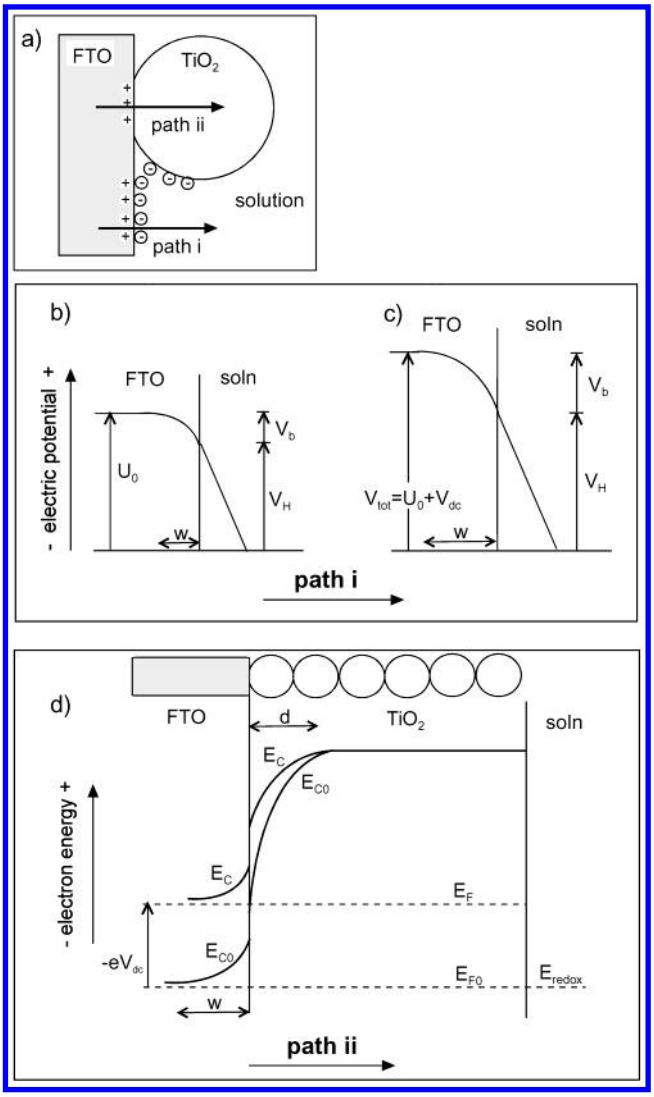

Figure 6. (a) Scheme of the three-phase contact: the FTO substrate, the porous TiO_2 network, and the electrolyte. (b) Potential distribution at the FTO/electrolyte interface at equilibrium in the dark: U_0, total potential drop ($U_0 = -$flatband potential vs U_{redox}); V_b, band-bending in FTO; V_H, Helmholtz potential drop. (c) Effect of an applied potential V_{dc}. (d) Energy diagram of the FTO/TiO_2 interface: E_c, conduction band of TiO_2 and FTO; E_F, Fermi level.

The model developed here allows one to extract relevant parameters such as U_0 and U_1 from interference reflection experiments [$(\Delta R/R)^2$ vs V_{dc} plots].

Figure 6 shows the potential distribution at the triple contact (FTO, TiO_2, electrolyte), both under dark, equilibrium conditions ($E_F = E_{redox}$) and under an applied external potential, V_{dc}, as explained previously.[2,10] A recent study[10] shows that the exposed area of the substrate is relatively very large with respect to the area covered by TiO_2 nanoparticles. Therefore, we assume in the following that the interference reflectance signal is controlled by the FTO/electrolyte interface (path i). In section 5 we will discuss in a more general way the simultaneous variation of the potential distribution in both pathways, i and ii.

Let U_0 represent the Galvani potential of the electrolyte with respect to the equilibrium Galvani potential of the FTO substrate in the dark, i.e., the total potential difference across the FTO/electrolyte interface when the system remains at equilibrium. Under application of a dc potential, V_{dc}, and on the assumption that the counter electrode potential remains pinned at the redox electrolyte level, the conduction band in the bulk of the FTO is shifted positively by the same amount, V_{dc}, ($V_{tot} = U_0 + V_{dc}$). According to the present study, it can be claimed that the FTO substrate does not show metallic behavior, since the applied potential drops partially both at the Helmholtz layer (V_H) and at the depletion layer (V_b), as shown in Figure 6c.

Since no reference electrode exists in the usual configuration of the DSSC,[22] we take the electrolyte redox potential, E_{redox}, as a reference potential, so that the flatband potential of the FTO becomes $V_{fb} = -U_0$. U_0 represents the shift of the Fermi level when the two separated phases, FTO and redox electrolyte, equilibrate in the dark ($E_F = E_{F0}$), or in other words, the difference of the work function of both phases.

The total potential drop, V_{tot}, is divided in two parts: $V_{tot} = V_b + V_H$, where V_H is the potential difference across the Helmholtz layer, and V_b is the potential drop in the space charge region (band-bending). The width of the depletion region is

$$w = \left(\frac{2\epsilon_r\epsilon_0 V_b}{N_d e}\right)^{1/2} \tag{10}$$

The potential distribution at the FTO depletion layer can be described by the expression

$$V(z) = V_{tot} - \frac{N_d e}{\epsilon_r\epsilon_0}\{z - w\}^2 \tag{11}$$

where z is the distance from the surface of the substrate. Thus, the electrical field can be written as

$$E(z) = \frac{N_d e}{\epsilon_r\epsilon_0}\{z - w\} \tag{12}$$

The charge/area in the depletion layer is $Q_b = N_d w e$. Assuming a constant value for C_H, the charge accumulated in the electrolyte side of the FTO surface will be $Q_H = C_H V_H$. On the other hand, according to the charge-neutrality constraint (i.e., $Q_b = Q_H$) it can be written that

$$4U_1V_b = V_H^2 \tag{13}$$

where U_1 is defined in eq 1. Therefore,

$$V_{tot} = V_b + V_H = V_b + 2(U_1V_b)^{1/2} \tag{14}$$

and solving these last two equations for V_H, we get an expression for the potential drop at the Helmholtz layer, V_H, as a function of the applied bias, V_{dc}:

$$V_H = 2U_1\left[\left(1 + \frac{V_{dc} + U_0}{U_1}\right)^{1/2} - 1\right] \tag{15}$$

By combining eqs 13 and 15 an expression for V_b as a function of V_{dc} can be obtained.

The modulation of the applied dc potential with amplitude $\Delta V_{dc} = V_{ac}$ induces a modulation of the electrical field in the FTO substrate, and therefore in its complex refraction index,

$$\hat{n}_2 = n_2 + i\frac{\lambda}{4\pi}\alpha_2(\lambda) \tag{16}$$

From the experimental results in Figure 4, it is seen that the applied potential only alters the amplitude and not the position of the ΔR spectrum. This is just an indication that the applied electric field only affects the imaginary part of the refraction index. According to Nonomura et al.,[18] the influence of the electrical field on the back-surface reflected electroabsorption

is described by a quadratic dependence of the absorption coefficient on the local field,

$$\hat{n}_2 = n_2 + i\frac{\lambda}{4\pi}\alpha_{20}(\lambda) + i\frac{\lambda}{4\pi}C(\lambda)E^2 \qquad (17)$$

where α_{20} is the absorption coefficient in the absence of a field. From eq 17 results the modulated component of the refraction index, eq 6. The modulated electric field component takes the form

$$\Delta E = \frac{\partial E}{\partial V_{dc}}\Delta V_{dc} = \frac{\partial E}{\partial V_b}\frac{\partial V_b}{\partial V_{dc}}V_{ac} \qquad (18)$$

As shown in eq 7 the modulated reflectivity ΔR contains two contributions, and we have assumed that the variation of optical path induced by the variation of the refraction index gives the dominant one. According to eq 9 this contribution is proportional to the integral of $\Delta\hat{n}_2$, eq 6, over the space charge region ($0 \le z \le w$). From eq 12 we get

$$\frac{\partial E}{\partial V_b} = -\frac{1}{w} \qquad (19)$$

and from eqs 13 and 15 we obtain

$$\frac{\partial V_b}{\partial V_{dc}} = \frac{V_H}{V_H + 2U_1} = \frac{2V_b}{V_{tot} + V_b} \qquad (20)$$

Substituting eqs 19 and 20 in eq 18 and integrating $E\Delta E$ over the whole space charge region, we get

$$\int_0^w E\Delta E\, dz = \frac{N_D e}{2\epsilon_r\epsilon_0}w(V_b)\frac{V_H}{V_H + 2U_1}V_{ac} \qquad (21)$$

Therefore, using eq 10 and noting that $V_b = V_{dc} + U_0 - V_H$, we arrive at

$$\Delta R = K\frac{\int \Delta\hat{n}_2\, dz}{\Delta V_{dc}} = iK\frac{\lambda}{2\pi}C(\lambda)\left[\frac{N_D e}{2\epsilon_r\epsilon_0}(V_{dc} + U_0 - V_H)\right]^{1/2}\frac{V_H}{V_H + 2U_1} \qquad (22)$$

so that

$$\left(\frac{\Delta R}{R}\right)^2 = B(V_{dc} + U_0 - V_H)\left(\frac{V_H}{V_H + 2U_1}\right)^2 \qquad (23)$$

where K are B are independent of V_{dc}. Equations 15 and 23 constitute a complete formulation for estimating the dependence of the modulated reflectivity amplitude on the bias potential, V_{dc}, at a fixed wavelength. Interestingly, U_0 and U_1 appear as separated parameters. Figure 7 illustrates the dependence of $(\Delta R/R)^2$ on V_{dc} according to eq 23. At very positive V_{dc} values, such that $V_H \gg U_1$ and $V_{dc} \gg V_H$, the model predicts a nearly linear dependence of $(\Delta R/R)^2$ with respect to V_{dc}. Also remarcable is the extraordinary sensitivity of $\Delta R/R$ to the value of C_H.

A fit of the experimental data of $(\Delta R/R)^2$ vs V_{dc} from eq 23 is shown in Figure 5 (line). The fit is almost perfect, with a correlation factor 0.9990, and leads to the following values of adjustable parameters: $U_0 = 1.6$ V, $B = 8.53 \times 10^{-7}$ V^{-1} and $U_1 = 0.21$ V. From these parameters and values of $N_d = 10^{21}$ cm^{-3} and $\epsilon_r = 9$, eq 1 leads to a reasonable value of the Helmholtz capacitance, $C_H = 17.4$ μF cm^{-2}.

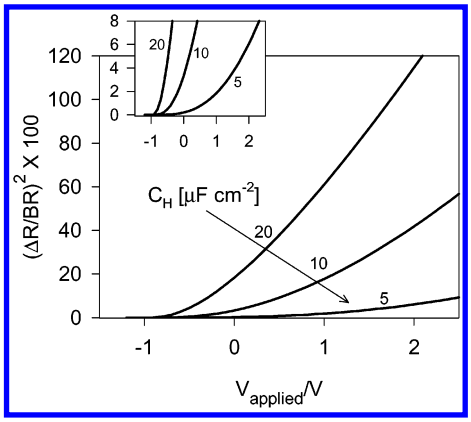

Figure 7. Plots of $(\Delta R/R)^2$ vs V_{dc} according to eq 23, for $U_0 = -1.6$ V vs U_{redox}, $N_d = 10^{21}$ cm^{-3}, $\epsilon_r = 9$ and different values of C_H corresponding to $U_1 = 0.16$, 0.63, and 2.5 V. The inset shows the behavior of the curves at low values of $(\Delta R/R)^2$.

5. Discussion

We have shown experimental evidence that the interference reflection spectra is controlled by the FTO/electrolyte interface. Let us now consider the implications of this result for DSSCs. With this purpose we will consider toguether the FTO/electrolyte and TiO_2/electrolyte interfaces. In Figure 6 these interfaces were represented as independent, but now we emphasize that the potential distribution in both interfaces should be correlated, as indicated in Figure 8. Under illumination the Fermi level both in FTO and TiO_2 is determined by the accumulation of photogenerated electrons in the conduction band of the nanostructured TiO_2 film, which determines the open-circuit voltage, $eV_{oc} = E_F^* - E_{redox}$. In addition, we assume that the band-bending in the FTO is homogeneous and determined by the FTO/electrolyte interface, as discussed before. The modification in the band-bending in the TiO_2 under photon irradiation will be discussed below.

Figure 9 shows the actual structure of the DSSC back contact, FTO/TiO_2 interface according to the model of the potential distribution outlined above. We can see in Figure 9a the situation under equilibrium, dark conditions, that follows from the experimental data. For $U_0 = 1.6$ V, $N_d = 10^{21}$ cm^{-3}, $\epsilon_r = 9$, and $C_H = 17.4$ μF cm^{-2}, at the FTO side of the contact we have $V_b = V_H = 0.8$ V, while at the TiO_2 side, for $E_c - E_{redox} = 0.95$ eV,[5] it is $(E_c - E_{redox})/e - V_b = 0.15$ V. For simplicity, a possible band offset between the materials has been neglected here (see Figure 6d).

The fact that $U_0 = 1.6$ V is surprising, since the work function of both the FTO and the I^-/I_3^- redox couple (in aqueous solution) are relatively close to each other, viz. $\phi(FTO) = 4.7$ eV and $\phi(I^-/I_3^-) = 4.85$ eV (vs electron at rest in a vacuum), which imply $U_0 \approx 0.15$ V when the two systems reach equilibrium in the dark, as confirmed by electrochemistry measurements.[15] A part of this difference could be due to the modification of the redox potential of the electrolyte (I^-/I_2 redox couple) due to the organic solvent used in the DSSC. It must be also emphasized that the results shown in Figure 7 were not obtained under equilibrium but under DSSC working conditions (150 W Xe lamp illumination and variable potential bias). A similar effect, due to a change of the apparent flatband potential, has been reported in unsensitized nanostructured TiO_2 in contact with water, under UV irradiation.[16] However, this effect was

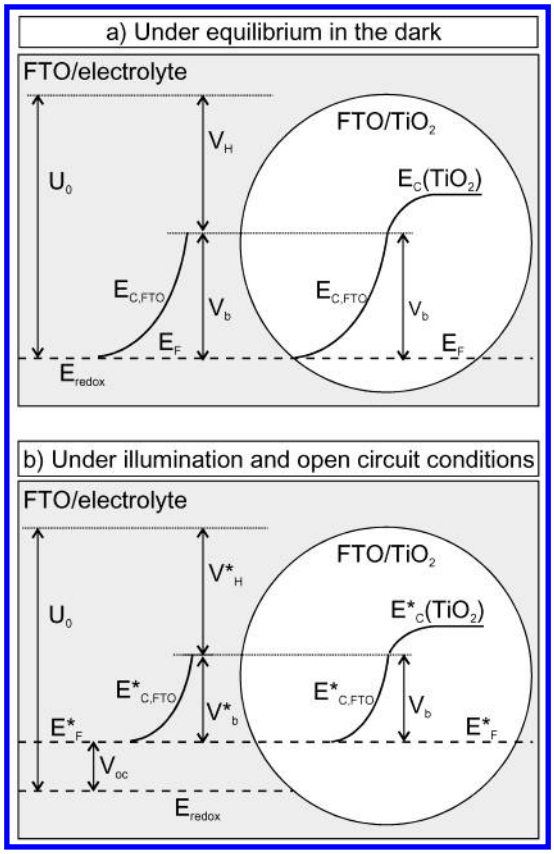

Figure 8. Energy diagram of the FTO conducting substrate in contact with the electrolyte and with a TiO_2 nanoparticle, showing the two regions indicated in Figure 6a: (a) under equilibrium in the dark and (b) under illumination and open circuit conditions. U_0, potential drop across the interface under equilibrium in the dark ($-U_0$ = flatband potential vs U_{redox}); V_b, bandbending in FTO; V_H, Helmholtz potential; E_c, lower edge of the conduction band; E_F, Fermi level.

attributed to the accumulation of photogenerated valence band holes at surface states, which, obviously, is not possible in a DSSC.

In the model outlined in the previous section, we have adopted the hypothesis that the modification of the barrier at the FTO surface, with respect to the dark equilibrium properties, is determined by the position of the Fermi level (Figures 8 and 9). This is based on the commonly accepted assumption in solar cell and semiconductor device theories that the equilibrium properties of Schottky barriers at depletion zones are not affected by the pass of an electron current through them. So, it may be assumed that the disparity of the FTO flatband potential obtained in the illuminated DSSC with respect to the expected thermodynamic, equilibrium value can be explained as due to some failure of the Schottky model. For instance, the assumption of common vacuum levels at the FTO/electrolyte interface is doubtful, due to the presence of an interfacial dipole associated with electron trapping at surface states. On the other hand, it should be taken into account that the actual shape of the interfacial, potential barrier can be strongly affected by photoinjected electrons. Further research seems therefore necessary in order to clarify the origin of this feature.

Despite this, it can be illustrative to discuss the implications of $U_0 = 1.6$ V on the maximum attainable photovoltage of a DSSC. Under illumination and open circuit conditions E_F moves up and a photovoltage is developed ($eV_{oc} = E_F^* - E_{redox}$). In principle, the maximum photovoltage is theoretically attained when $E_F^* = E_c^*(TiO_2)$ (i.e., $eV_{oc,max} = E_c^*(TiO_2) - E_{redox}$). However, in the case where E_c^*(FTO, surface) $- E_c^*(TiO_2$, bulk) > 0, a barrier appears at FTO/TiO_2 interface, hindering the movement of dye photoinjected electrons from the TiO_2 to the FTO. Therefore, the actual, maximum attainable photovoltage is conditioned by the value of E_c^*(FTO, surface). This situation is shown in Figure 9b. Since

$$V_{oc} = U_0 - V_b^* - V_H^* \tag{24}$$

both V_b^* and V_H^* decrease as V_{oc} increases, so that the actual, maximum attainable photovoltage corresponds to the minimum values of V_b^* and V_H^*. Hence,

$$V_{oc,max} = U_0 - V_{b,min}^* - V_{H,min}^* \tag{25}$$

with the condition that

$$V_{H,min}^* = U_0 - [E_c^*(TiO_2) - E_{redox}] \tag{26}$$

By combining eqs 13 and 26, and for values of $U_0 = -1.6$ V vs U_{redox}, $U_1 = 0.21$ V and $E_c^*(TiO_2) - E_{redox} = 1.1$ eV, which takes into account a TiO_2 band-edge shift of about 0.15 eV toward negative potential values due to accumulation of electrons at band gap surface states,[23] values $V_{H,min}^* = 0.5$ V

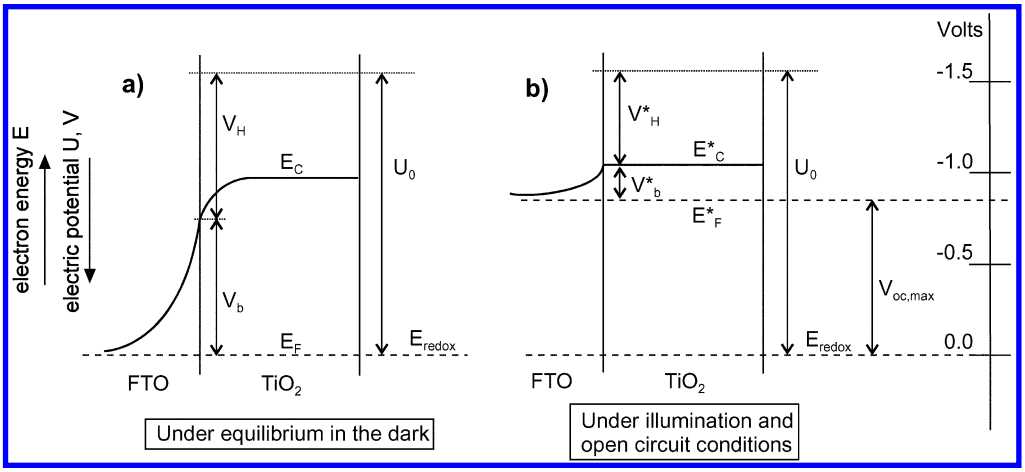

Figure 9. Structure of the potential barrier at the FTO/TiO_2 interface of the DSSC back contact, according to the data of Figure 6, under (a) thermal equilibrium in the dark and (b) open circuit conditions and an illumination flux giving rise to a maximum photovoltage ($V_{oc,max}$). This is reached for $E_c^*(FTO) = E_c^*(TiO_2)$. Any additional increase of the incident photon flux will produce a rise of the Fermi level at the TiO_2 but not at the FTO, so that the photovoltage $V_{oc} = (E_F^*(FTO) - E_{redox})/e$ does not further increase. The symbol (*) denotes values under illumination, nonequilibrium conditions.

and $V_{b,min}^* = 0.3$ V are obtained. It follows from eq 25 that a $V_{oc,max} = 0.8$ V, which is lower than $E_c^*(TiO_2) - E_{redox} = 1.1$ eV, is obtained. A further increase of the illumination intensity should produce a rise of the Fermi level in the TiO_2, but not in the FTO, so that the photovoltage cannot further increase.

Summing up, the actual limit of the maximum attainable DSSC photovoltage is not given by the difference between the energies of the bottom of the TiO_2 conduction band under illumination (E_c^*) and the electrolyte redox potential ($E_c^* - E_{redox} = 1.1$ eV), as usually assumed. The existence in the FTO substrate of a depletion layer with characteristics (heigth and position) that are very sensitive to Fermi level energy and the very negative FTO flatband potential ($U_0 = -1.6$ V vs U_{redox}) under illumination working conditions of the DSSC leads to a considerable diminution of $V_{oc,max}$. In fact, a potential barrier should appear at the FTO/TiO_2 interface for values of (E_F(FTO) $- E_{redox}$) > 0.8 V. This barrier would hinder the transfer of dye-photoinjected electrons from the TiO_2 to the FTO at the back contact, producing a diminution of $V_{oc,max}$ from the 1.1 V theoretical value to about 0.8 V. In support of this hypothesis is the experimental fact that photopotentials higher than about 0.8 V have never been reported for a conventional (untreated) DSSC.[23,24]

Acknowledgment. J.B. acknowledges support of this work by Ministerio de Ciencia y Tecnología of Spain under project BFM2001-3604.

References and Notes

(1) Turrión, M.; Macht, B.; Tributsch, H.; Salvador, P. *J. Phys. Chem. B* **2001**, *105*, 9732.
(2) Bisquert, J.; Garcia-Belmonte, G.; Fabregat Santiago, F. *J. Solid State Electrochem.* **1999**, *3*, 337.
(3) van de Krol, R.; Goossens, A.; Schoonman, J. *J. Electrochem. Soc.* **1997**, *144*, 1723.
(4) van de Lagemaat, J.; Park, N.-G.; Frank, A. J. *J. Phys. Chem. B* **2000**, *104*, 2044.
(5) Cahen, D.; Hodes, G.; Grätzel, M.; Guillemoles, J. F.; Riess, I. *J. Phys. Chem. B* **2000**, *104*, 2053.
(6) Schwarzburg, K.; Willig, F. *J. Phys. Chem. B* **1999**, *28*, 5743.
(7) Huang, S. Y.; Schilchthörl, G.; Nozik, A. J.; Grätzel, M.; Frank, A. J. *J. Phys. Chem. B* **1997**, *101*, 2576.
(8) Kron, G.; Egerter, T.; Werner, J. H.; Rau, W. *J. Phys. Chem. B* **2003**, *107*, 3556.
(9) Zhu, K.; Schiff, E. A.; Park, N. G.; van de Lagemaat, J.; Frank, A. J. *Appl. Phys. Lett.* **2001**, *80*, 685.
(10) Fabregat-Santiago, F.; Garcia-Belmonte, G.; Bisquert, J.; Bogdanoff, P.; Zaban, A. *J. Electrochem. Soc.* **2003**, *150*, E293.
(11) de Gryse, R.; Gomes, W. P.; Cardon, F.; Vennik, J. *J. Electrochem. Soc.* **1975**, 711.
(12) Pettinger, B.; Schöppel, H.-R.; Yokoyama, T.; Gerischer, H. *Ber. Bunsen-Ges. Phys. Chem.* **1974**, *78*, 1024.
(13) Armstrong, N. R.; Lin, A. W. C.; Fujihira, M.; Kuwana, T. *Anal. Chem.* **1976**, *48*, 741.
(14) van den Meerakker, J. E. A. M.; Meulenkamp, E. A.; Scholten, M. *J. Appl. Phys.* **1993**, *74*, 3282.
(15) Peter, L. M.; Duffy, N. W.; Wang, R. L.; Wijayantha, K. G. U. *J. Electroanal. Chem.* **2002**, *524−525*, 127.
(16) Hagfeldt, A.; Björkstén, U.; Grätzel, M. *J. Phys. Chem.* **1996**, *100*, 8045.
(17) Frova, A.; Migliorato, P. *Appl. Phys. Lett.* **1969**, *15*, 406.
(18) Nonomura, S.; Okamoto, H.; Hamakawa, Y. *Appl. Phys. A* **1983**, *32*, 31.
(19) Blackwood, D. J.; Peter, L. M. *Electrochim. Acta* **1989**, *35*, 1073.
(20) Born, M.; Wolf, E. *Principles of Optics*; Pergamon Press: New York, 1980.
(21) Mattews, C. G.; Ord., J. L.; Wang, W. P. *J. Electrochem. Soc.* **1983**, *130*.
(22) Zaban, A.; Zhang, J.; Diamant, Y.; Melemed, O.; Bisquert, J. *J. Phys. Chem. B* **2003**, *107*, 6022.
(23) Schlichthörl, G.; Huang, S. Y.; Sprague, J.; Frank, A. J. *J. Phys. Chem. B* **1997**, *101*, 8141.
(24) Fisher, A. C.; Peter, L. M.; Ponomarev, E. A.; Walker, A. B.; Wijayantha, K. G. U. *J. Phys. Chem. B* **2000**, *104*, 949.